Supplementary Information

for

Dual Functionalization of UiO-66-NH_2 for Efficient and Selective Au(III) Adsorption: Synergistic Effect of Electrostatic and Coordination Interactions

Chang Zhang,[a] Xinru lv,[a] Zhouyi Su,[a] Sheng Zhang,[a] Xuhai Liu,[a] Xusheng Wang,[b] Feng Yang,[c] Xiognfei Wang,[d] Huaixia Zhao, *[a] Yangxin Wang*[a]

[a] College of Materials Science and Engineering, Nanjing Tech University, Nanjing 211816, P. R. China

[b] Institute of Functional Porous Materials, School of Materials Science and Engineering, Zhejiang Sci-Tech University, Hangzhou 310018, P. R. China

[c] College of Chemistry, Sichuan University, Chengdu 610064, P. R. China

[d] Nantong Guixin Technology Co., LTD, Nantong 226412, P. R. China

Corresponding authors:

Yangxin Wang, yangxin.wang@njtech.edu.cn;

Huaixia Zhao, zhaohx@njtech.edu.cn

1. Materials

Sodium chloride, thiourea, and tetrachloroauric acid ($HAuCl_4 \cdot 4H_2O$) were purchased from National Pharmaceutical Group Co., Ltd (Beijing, China). Azobisisobutyronitrile (AIBN), 2-amino benzene dicarboxylic acid ($H_2BDC\text{-}NH_2$), and glyoxal (40 wt% in H_2O) were purchased from Aladdin Chemistry Co., Ltd (Shanghai, China). N,N-dimethylformamide (DMF) was purchased from Wuxi Yasheng Chemical Engineering Co., Ltd (Wuxi, China). Thiosemicarbazide (TSC), 3-Bromopropylamine hydrobromide (BPA), and 1-vinylimidazole were purchased from Adamas Chemical

Reagent Co., Ltd (Shanghai, China). Zirconium chloride ($ZrCl_4$) was purchased from InnoChem Science & Technology Co., Ltd (Beijing, China). Ethylene glycol dimethacrylate (EDMA) was purchased from Energy Chemical Reagent Co., Ltd (Shanghai, China). Hydrochloric acid was purchased from Huishi Chemical Reagent Co., Ltd (Nanjing China). Acetic acid was purchased from Meryer Chemical Reagent Co., Ltd (Shanghai, China). The amine-terminated imidazolium ionic liquid (AVIM) was synthesized according to our previously reported method [1].

2. Instruments

Fourier-transform infrared (FTIR) spectra were obtained using KBr pellets with Nicolet iS 5 FTIR spectrometer (Thermo Fisher Scientific, USA), Powder X-ray diffraction (PXRD) patterns were recorded in the range of $2\theta = 5\sim70°$ on a desk X-ray diffractometer (SmartLab-9kW, Rigaku Electric Co., Ltd, Japan). SNE-4500M Plus (SEC e-beam pioneer, China) was employed to record the scanning electron microscopy (SEM) images. Inductively coupled plasma-atomic emission spectroscopy (ICP-AES) measurements were carried out to measure Au(III) content on an Avio 200 optical emission spectrometer (PerkinElmer, USA). Elemental analysis was performed on Vario EL cube (Elementar, Germany). X-ray photoelectron spectroscopy (XPS) characterization was performed on ESCALAL 250Xi (Thermo Fisher Scientific, USA). Zeta potentials were measured on a Zeta potential analyzer (Malvern Zetasizer Nano ZS90, UK). N_2 adsorption experiments were performed on an automatic specific surface area and porosity analyzer (Micromeritics APSP 2460, USA) under 77 K. The samples were degassed at 120°C for 8 h before test. The Brunauer-Emmett-Teller (BET) method was used to calculate the specific surface area based on the adsorption data in the partial pressure of $0.05 < P/P_0 < 0.35$. Non-local density functional theory (NLDFT) was applied to analyzed pore size distribution.

3. Preparation of UiO-66-NH_2

UiO-66-NH_2 was prepared according to a reported method with modification[2]. Typically, $ZrCl_4$ (0.932 g, 4 mmol) and H_2BDC-NH_2 (0.725 g, 4 mmol) were dissolved

in DMF (160 mL) at room temperature. After that, acetic acid (11.4 mL) was added to the solution as a modulator. The mixture was transferred into a Teflon lining stainless steel reaction kettle and heated at 120°C for 24 h. After the solvothermal reaction, the resulting solid was separated by centrifugation and washed with DMF and ethanol repeatedly. Finally, the product was dried under vacuum at 60°C for 6 h.

4. Adsorption experiments

The concentration of Au(III) in aqueous solution was determined using ICP-AES. All adsorption experiments were performed in triplicate. The adsorption capacity (q_t) and removal efficiency (R_t) are calculated based on the following equations[3, 4]:

$$q_t = （c_0 - c_t） \times \frac{V}{m} \qquad \textbf{Equation S1}$$

$$R_t = \frac{c_0 - c_t}{c_0} \times 100\% \qquad \textbf{Equation S2}$$

where q_t (mg/g) is the adsorption amount of Au(III) after contact time t, c_0 (mg/L) is the initial concentration of Au(III), c_t (mg/L) is the Au(III) concentration at contact time t, m (g) is the quantity of added adsorbent, and V (L) represents the solution volume.

The Langmuir (**Equation S3)** and Freundlich (**Equation S4**) adsorption isotherms are represented as follows, respectively[5]:

$$q_e = \frac{K_L q_m c_e}{1 + K_L c_e} \qquad \textbf{Equation S3}$$

$$q_e = K_F c_e^{\frac{1}{n}} \qquad \textbf{Equation S4}$$

where q_e (mg/g) and c_e (mg/L) represent the adsorption capacity and the concentration of Au(III) at adsorption equilibrium. q_m (mg/g) represents the theoretical maximum adsorption capacity. K_L (L/mg) is the constant of the Langmuir model which relates to the energy of the biding sites and affinity to adsorption. K_F (mg/g) is a constant relates to adsorption capacity and adsorption intensity, and 1/n is the Freundlich constant indicating the extent of nonlinearity between the solution concentration and adsorption capacities.

The pseudo-first-order (PFO) (**Equation S5**) and pseudo-second-order (PSO) (**Equation S6**) kinetic model equations are expressed as follows[6]:

$$\ln\left(q_e - q_t\right) = lnq_e - k_1 t \qquad \textbf{Equation S5}$$

$$\frac{t}{q_t} = \frac{1}{k_2 {q_e}^2} + \frac{t}{q_e} \qquad \textbf{Equation S6}$$

where k_1 (min^{-1}) and k_2 (g/(mg·min)) represent the rate constant of PFO and PSO model, respectively. q_e (mg/g) and q_t (mg/g) represent the adsorption capacity of Au(III) at adsorption equilibrium and contact time t (min), respectively.

The Gibbs free energy change (ΔG^0), enthalpy change (ΔH^0), and entropy change (ΔS^0) for the adsorption of Au(III) on UiO-66-AVIM-TSC were calculated according to the Equations as follows [7]:

$$K_d = \frac{q_e}{c_e} \qquad \textbf{Equation S7}$$

$$\Delta G = -RTlnK_d \qquad \textbf{Equation S8}$$

$$lnK_d = \frac{\Delta S}{R} - \frac{\Delta H}{RT} \qquad \textbf{Equation S9}$$

where K_d denotes the distribution coefficient of the adsorbent equal to q_e/c_e, T (K) signifies the temperature of adsorption in Kelvin, and R is the universal gas constant (8.314 J/(mol·K)). ΔH^0 and ΔS^0 are calculated according to the slope and intercept of the linear plot of $\ln(K_d)$ *vs*. 1/T (**Figure S1**).

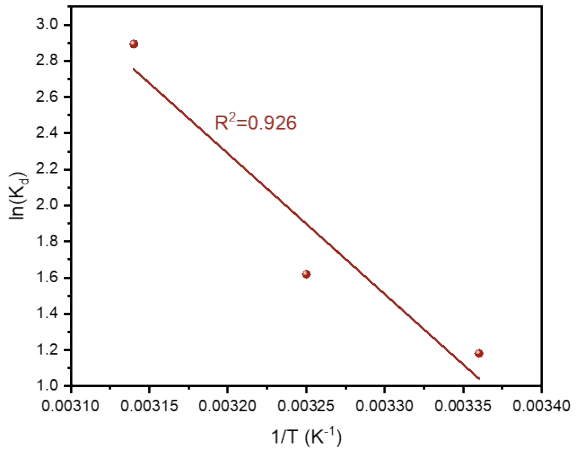

Figure S1. The linear plot of $\ln(K_d)$ *vs.* 1/T to determine ΔH^0 and ΔS^0.

5. Determination of point of zero charge (PZC)

PZC of UiO-66-AVIM-TSC was measured following a reported protocol[8]. Initially, UiO-66-AVIM-TSC (10 mg) was added into NaCl aqueous solution (0.1 M, 15 mL) with pH values ranging from 1.0 to 11.0. After shaken at room temperature for sufficient time until pH values reach constant, the change of pH values (Δ pH) of the NaCl solutions were plotted against the initial pH values (pH_i). The PZC was determined as the pH_i corresponding to the position at where $\Delta pH = 0$.

6. Reusability test

UiO-66-AVIM-TSC (20 mg) was added into 30 mL $HAuCl_4$ solution (100 mg/L). After shaken for sufficient time until adsorption reaches equilibrium, the residual concentration of Au(III) was measured by ICP-AES to calculate the adsorption capacity and removal efficiency. The used UiO-66-AVIM-TSC was separated through centrifugation, and rinsed with thiourea (10 wt.%) and HCl (5 wt.%) solution to remove the adsorbed Au(III). After further washed with deionized water, the regenerated UiO-66-AVIM-TSC was dried under 60°C in vacuum. After this, the regenerated UiO-66-AVIM-TSC was subjected to the next cycle of adsorption experiment.

7. Selectivity test

UiO-66-AVIM-TSC (10 mg) was added into 15 mL aqueous solution (pH = 3.0) containing $HAuCl_4$, $Zn(NO_3)_2$, $CuCl_2$, $AlCl_3$, $MgSO_4$, LiCl, and $K_2Cr_2O_7$. After the mixture was shaken for sufficient time until adsorption reaches equilibrium, residual concentration of these metal ions was measured. The distribution coefficient (K_D) and selectivity coefficient (K) were calculated according to following equations [9]:

$$K_D = \frac{q_e}{c_e}$$

$$K = \frac{K_{D(Au^{3+})}}{K_{D(coexisting\ ions)}}$$

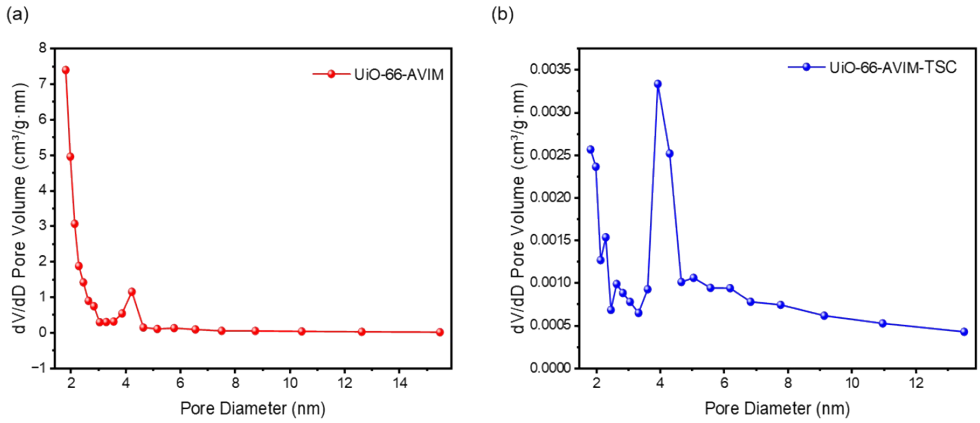

Fig. S2 Pore size distribution of (a) UiO-66-AVIM and (b) UiO-66-AVIM-TSC.

Table S1. A comparison of adsorption capacity of Au(III) on various adsorbents

Entry	Adsorbent	q_m (mg/g)	Ref
1	MP@[Chi-CPTMS-SiO_2]	112	[10]
2	ZT-MOFs	333.34	[11]
3	APS-LCP	261.36	[12]
4	UiO-66-MTD	301.5	[13]
5	AIAC	191.92	[14]
6	azo-HNTA-MIL-101(Al)	77.4	[15]
7	UIO-67-$(NH_2)_2$	482	[16]
8	PCN-224	650	[17]
10	UiO-66-AVIM-TSC	220.26	This work

Reference

1. X. Li, Z. Wang, W. Bi, F. Yang, X. Wang, Y. Wang and H. Zhao, Polymer, 2024, 309, 127465.
2. S. Li, F. Feng, S. Chen, X. Zhang, Y. Liang and S. Shan, Ecotoxicology and Environmental Safety,

2020, 194, 110440.
3. Y. Xiang, C.-Y. Cheng, M.-H. Liu, W.-C. Bai, Z.-X. Zang, L. Xu, Y. Yu and G.-J. Liu, Separation and Purification Technology, 2024, 335, 126131.
4. B. Wang, Y. Ma, W. Xu and K. Tang, J Hazard Mater, 2023, 451, 131051.
5. Y. Geng, J. Li, W. Lu, N. Wang, Z. Xiang and Y. Yang, Chemical Engineering Journal, 2020, 381, 122627.
6. Y. Xiang, X. Chen, C. Cao, S. Ding, L. Xu and G. Liu, Reactive and Functional Polymers, 2020, 154, 104637.
7. A. M.E.H, X. Y. Mbianda, A. F. Mulaba-Bafubiandi and L. Marjanovic, Hydrometallurgy, 2013, 140, 1-13.
8. S. K. Samanta, B. Mandal and T. Tripathy, Journal of Applied Polymer Science, 2022, 139, e52465.
9. C. Wang, G. Lin, J. Zhao, S. Wang and L. Zhang, Chemical Engineering Journal, 2020, 388, 124221.
10. N. Nuryono, D. Miswanda, S. C. W. Sakti, B. Rusdiarso, P. A. Krisbiantoro, N. Utami, R. Otomo and Y. Kamiya, Materials Chemistry and Physics, 2020, 255, 123507.
11. Z. Huang, M. Zhao, S. Wang, L. Dai, L. Zhang and C. Wang, Journal of Molecular Liquids, 2020, 298, 112090.
12. N. Saman, M. U. Rashid, J. W. P. Lye and H. Mat, Reactive and Functional Polymers, 2018, 123, 106-114.
13. C. Wang, G. Lin, J. Zhao, S. Wang, L. Zhang, Y. Xi, X. Li and Y. Ying, Chemical Engineering Journal, 2020, 380, 122511.
14. W. Wei, D. H. K. Reddy, J. K. Bediako and Y.-S. Yun, Chemical Engineering Journal, 2016, 289, 413-422.
15. A. Alharbi, Z. A. Al-Ahmed, N. M. El-Metwaly, A. Shahat and M. A. El-Bindary, Journal of Molecular Liquids, 2023, 369, 116498.
16. Z. Wang, G. Hu, C. Xia, X. Wang, H. He, Z. Nie, S. Wang and W. Li, Journal of Molecular Structure, 2025, 1321, 139873.
17. Y. Shu, Y. Chen, Q. Han, X. Liu, B. Liu and Z. Wang, ACS ES&T Engineering, 2023, 3, 1042-1052.